catalysts

MDPI

Article

Bi-Dentate Pyridyl Amine-Derived Complexes of Aluminium: Synthesis, Structure and ROP Capability

Shunsuke Sato [1], Ignas Motuzis [2], Mark R. J. Elsegood [2], Kotohiro Nomura [1,*] and Carl Redshaw [1,*]

[1] Department of Chemistry, Graduate School of Science, Tokyo Metropolitan University, 1-1 Minami Osawa, Hachioji 192-0397, Tokyo, Japan
[2] Chemistry Department, Loughborough University, Loughborough LE11 3TU, Leicestershire, UK; m.r.j.elsegood@lboro.ac.uk (M.R.J.E.)
* Correspondence: ktnomura@tmu.ac.jp (K.N.); credshaw@tmu.ac.jp (C.R.)

Abstract

The pyridylamines 2,6-$Me_2C_6H_3NHCR_2$-C_5H_5H-2 (R = H, L^1H; Me, L^2H) on treatment with Me_3Al (one equivalent) afforded the complexes $[Al(Me)_2(L^1)]$ (**1**) and $[Al(Me)_2L^2]$ (**2**), respectively. Use of excess L^1H led to $[Al(Me)(L^1)_2]$ (**3**). The molecular structures of **1**–**3** are reported, and the three complexes, as well as the parent compounds L^1H and L^2H, have been screened, in the presence of benzyl alcohol (BnOH), as catalysts for the ring opening polymerization (ROP) of ε-caprolactone and δ-valerolactone. Results revealed that these ROPs proceed in a controlled nature ($Đ \leq 1.33$ for ε-CL and ≤ 1.48 for δ-VL) in the process without catalyst deactivation, whilst the products formed were predominantly linear with OBn/OH end groups; L^1H and L^2H exhibited little or no activity.

Keywords: aluminium complexes; pyridyl anilines; solid-state structures; ring opening polymerization (ROP); cyclic esters

check for updates

Academic Editor: Francis Verpoort

Received: 30 October 2025
Revised: 10 November 2025
Accepted: 12 November 2025
Published: 1 December 2025

Citation: Sato, S.; Motuzis, I.; Elsegood, M.R.J.; Nomura, K.; Redshaw, C. Bi-Dentate Pyridyl Amine-Derived Complexes of Aluminium: Synthesis, Structure and ROP Capability. *Catalysts* **2025**, *15*, 1119. https://doi.org/10.3390/catal15121119

Copyright: © 2025 by the authors. Licensee MDPI, Basel, Switzerland. This article is an open access article distributed under the terms and conditions of the Creative Commons Attribution (CC BY) license (https://creativecommons.org/licenses/by/4.0/).

1. Introduction

Plastic pollution continues to be a significant global issue. With this in mind, much research is being devoted to exploring methods of accessing more environmentally friendly polymer products. One possibility that is attracting the attention of coordination chemists is the use of metal-catalysts in the ring opening polymerization (ROP) of cyclic esters [1–6]. In such a process, the ability to modify the ligation at the metal not only allows for control over the catalytic behaviour of the catalyst but can also greatly influence the resulting polymer properties. For such a catalytic system, it is useful to employ an earth-abundant element as the catalytic centre, with favourable toxicity and Lewis acidity. For example, metals such as magnesium, potassium, calcium, iron and zinc have received recent interest [4,7–11]. With this in mind, we and others have also been exploring the use of aluminium-based catalysts as the catalytic centre in ROP systems; aluminium is the third most abundant element in the earth's crust [12–22]. It is also noteworthy from previous studies that the use of chelate ligation is highly beneficial. In this study, we have chosen to employ two pyridylamines, namely 2,6-$Me_2C_6H_3NHCR_2$-C_5H_5N-2 (R = H, L^1H; Me, L^2H; Figure 1), as the precursors in order to employ 2-pyridylmethylanilido ligation at the aluminium centre (see **1**–**3**, Figure 2). The presence of the additional methyl in the backbone of L^2 (versus L^1) allows for a comparative study of the influence of the sterics associated with the ligand backbone. We note that L^1 has previously been employed with titanium and zirconium to form catalysts capable of *cis*-1,4-polymerization of 1,3-butadiene [23], and we have reported

that the use of ligation based on L^1 results in active ethylene dimerization/polymerization catalysts based on vanadium [24–26] and niobium [27]. Moreover, we note that pyridyl-alkylamide aluminium catalysts bearing naphthyl substituents (see **I** and **II**, Figure S1, SM) have been utilised for the ROP of ε-caprolactone (ε-Cl) [28], whilst catalysts bearing 2,6-diisopropylphenyl motifs at nitrogen centres are efficient for the block copolymerization of *L*-, *D*- and *rac*-lactide and ε-Cl (M = Zn, see **III**–**VI**, Figure S1, SM) [7], the ROP of ε-CL (M = Fe) [9], and for the ROP of δ-alkyl-δ-lactones and ε-lactones [10].

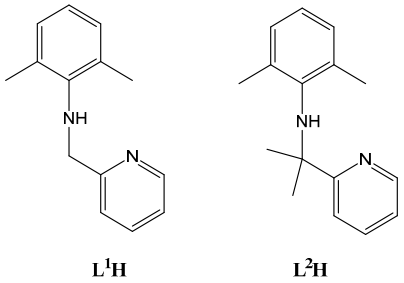

L^1H L^2H

Figure 1. Pyridylamines employed herein.

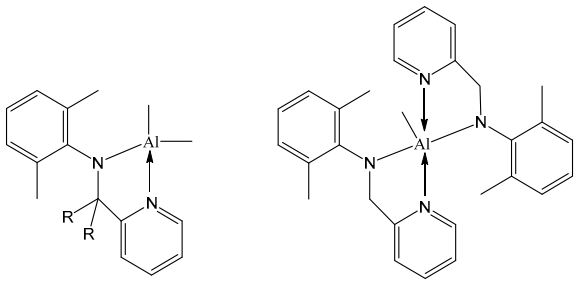

R = H (**1**), Me (**2**) [Al(Me)(L^1)$_2$] (**3**)

Figure 2. Complexes **1**–**3** reported herein.

2. Results and Discussion

2.1. Synthesis of Ligands and Complexes

The pyridylamine L^1H is readily available via reduction ($NaBH_4$) of the parent pyridylimine, as shown in Scheme 1 [24,25,29]. The complex [$Me_2Al(L^1)$] (**1**) is formed in good yield (>60%) following subsequent treatment with trimethylaluminium (1.2 equiv.) in refluxing toluene. The ^{1}H NMR spectrum of **1** is shown in Figure S2 in the SM.

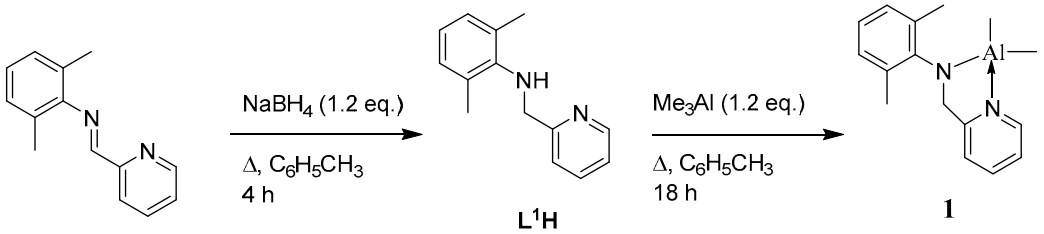

L^1H **1**

Scheme 1. Synthetic route to complex **1**.

In the case of L^2H, the synthetic method (Scheme 2) involves methyl transfer to the imine backbone via the use of trimethylaluminium. Such a method has proved fruitful in the formation of a variety of bi- and tridentate ligand sets [28,30–32]. Subsequent treatment of the pyridylamine with a second equivalent of trimethylaluminium affords [$Me_2Al(L^2)$] (**2**) in high yield (>90%). The ^{1}H NMR spectrum of **2** is shown in Figure S3 in the SM.

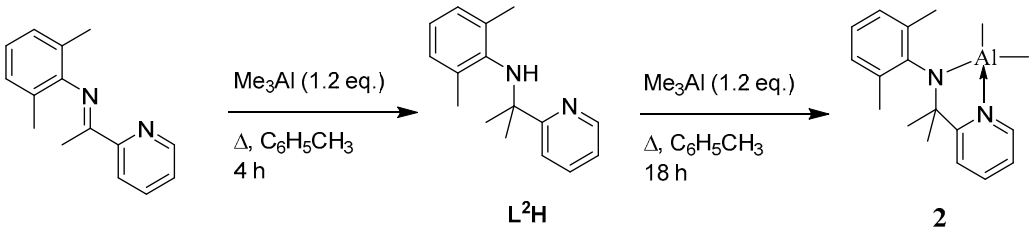

Scheme 2. Synthetic route to complex **2**.

We then decided to explore if changing the reaction stoichiometry would affect the nature of the product formed. Using L^1H as an example, it was found that on increasing the amount of L^1H to 2.1 equivalents (Scheme 3), work-up as for **1** afforded large colourless blocks in good yield (>90%). Spectroscopic and analytical data were consistent with the formula $[Al(Me)(L^1)_2]$ (**3**). The ^1H NMR spectrum of **3** is shown in Figure S4 in the SM.

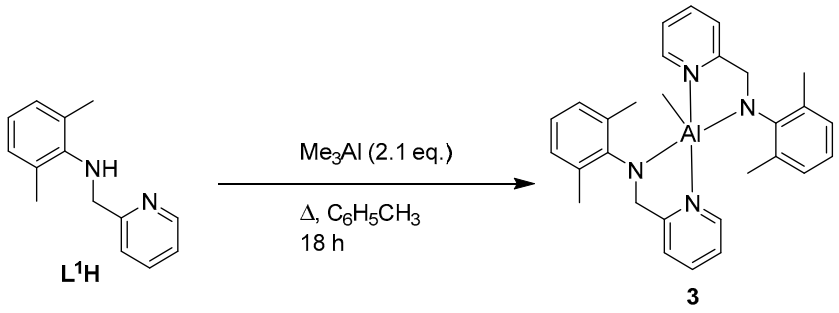

Scheme 3. Synthetic route to complex **3**.

2.2. Molecular Structures of Complexes

Single crystals of $[Al(Me)_2(L^1)]$ (**1**) suitable for X-ray crystallography were obtained from a saturated solution of acetonitrile on standing at 0 °C. A view of the molecular structure is shown in Figure 3 and in the packing is shown in Figure 4. Selected bond lengths and angles are given in the caption. There are two very similar molecules of **1** in the asymmetric unit. One chelating pyridylamine binds to an $AlMe_2$ motif, and the geometry at Al is distorted tetrahedral. The dihedral angles between ring systems in each molecule are N(1)/N(2)/C(1) > C(6) vs. C(7) > C(12) = 87.51(7)° and N(3)/N(4)/C(17) > C(22) vs. C(23) > C(28) = 80.08(7)°. Thus, in both cases they are almost perpendicular but a few degrees different. In the packing, molecules are arranged in anti-parallel stacks, as shown in Figure 3.

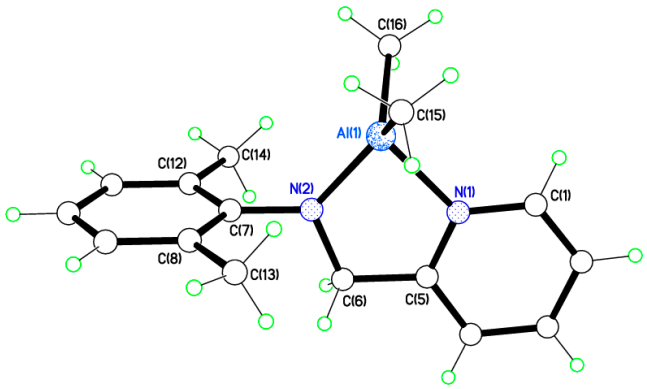

Figure 3. Molecular structure of $[Al(Me)(L^1)]$ (**1**), one of two very similar molecules in the asymmetric unit. Selected bond lengths (Å) and bond angles (°): Al(1)–N(1) 1.982(2), Al(1)–N(2) 1.838(2), Al(1)–C(15) 1.971(3); N(1)–Al(1)–N(2) 84.60(10), N(1)–Al(1)–C(15) 106.70(11).

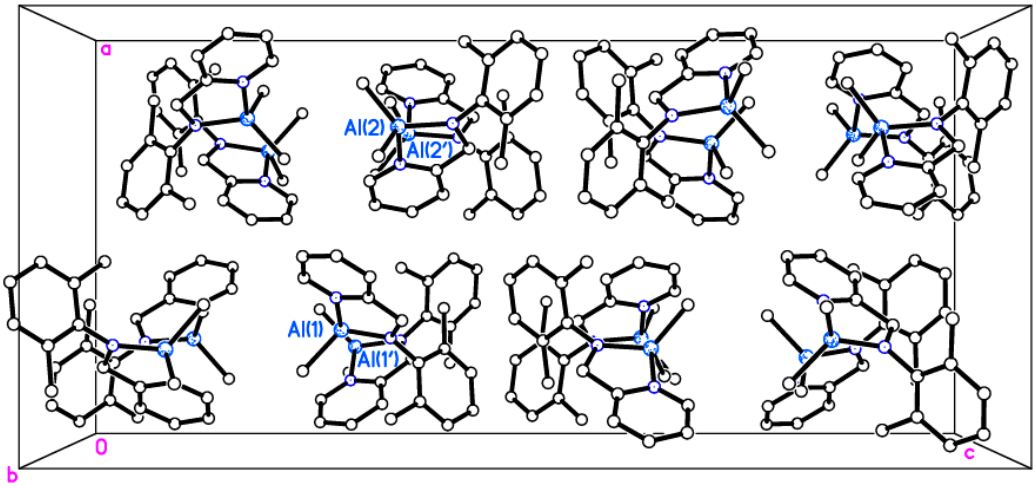

Figure 4. Packing in **1** with anti-parallel stacks.

In the case of **2**, crystals suitable for X-ray diffraction were again grown from acetonitrile at 0 °C. A view of the molecular structure is shown in Figure 5, with selected bond lengths and angles given in the caption. The presence of the extra methyl groups on the chelate backbone again led to the formation of a structure with one chelate bound to an $AlMe_2$ motif. We note that other studies have shown that changing the bulk of nitrogen-bound substituents in alkyl-2-pyridinamine diethyl aluminium complexes allows for monomer, dimer, or trimer formation [33]. Half of the molecule of **2** is unique. The atoms Al(1), N(1), C(1) > C(6), N(2), C(8) and C(11) are positioned on a mirror plane. The xylene group on N(2) is perpendicular to the pyridyl moiety of the chelating ligand to avoid Me group steric clashes.

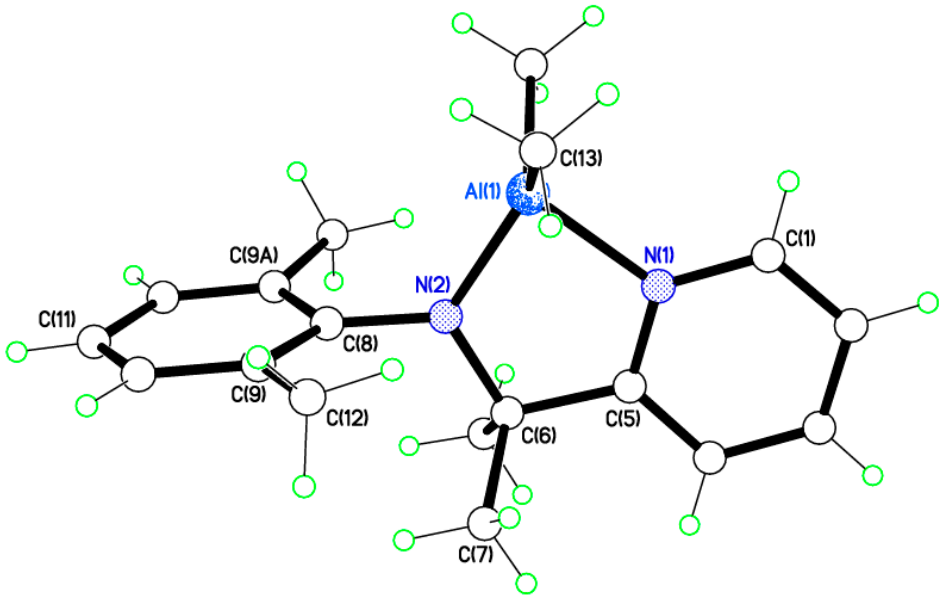

Figure 5. Molecular structure of $[Me_2Al(L^2)]$ (**2**). Selected bond lengths (Å) and bond angles (°): Al(1)–N(1) 1.9579(8), Al(1)–N(2) 1.8422(8), Al(1)–C(13) 1.9772(7); N(1)–Al(1)–N(2) 85.26(3), N(1)–Al(1)–C(13) 107.51(3).

In the packing (Figure 6), there is a weak H-bonding interaction from C(3)–H(3)···Al(1′) = 3.13 Å {symm. operator ′ = x, y, z + 1}, and this does seem to have pushed the Me groups on Al(1) slightly towards N(1) {See Figure S5 in the Supplementary Materials}. Molecules are arranged in anti-parallel stacks {See Figures 5 and S6}.

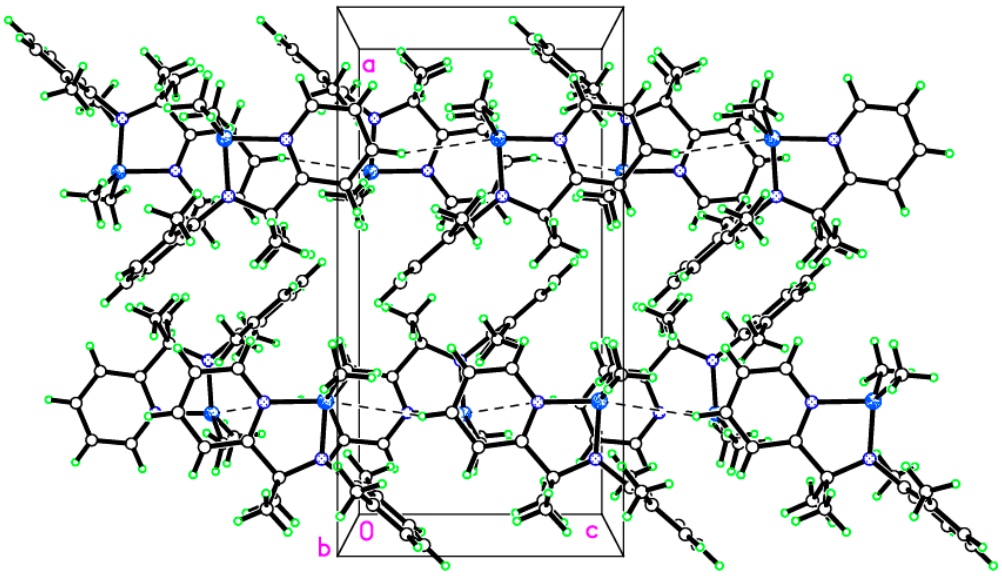

Figure 6. Weak C–H···Al interactions in the packing of **2** giving rise to chains in the *c* direction.

Single crystals of [Al(Me)(L^1)$_2$] (**3**) suitable for X-ray crystallography were obtained from a saturated solution of acetonitrile on standing at 0 °C. There is one molecule in the asymmetric unit (Figure 7) with the two pyridylamines binding to an AlMe centre which is closer to trigonal bipyramidal with N(1) and N(3) axial than to square-based pyramidal at the Al^{3+} ion, with τ = 0.82 [34]. The two chelating ligands coordinate anti-parallel to avoid methyl group steric clashes.

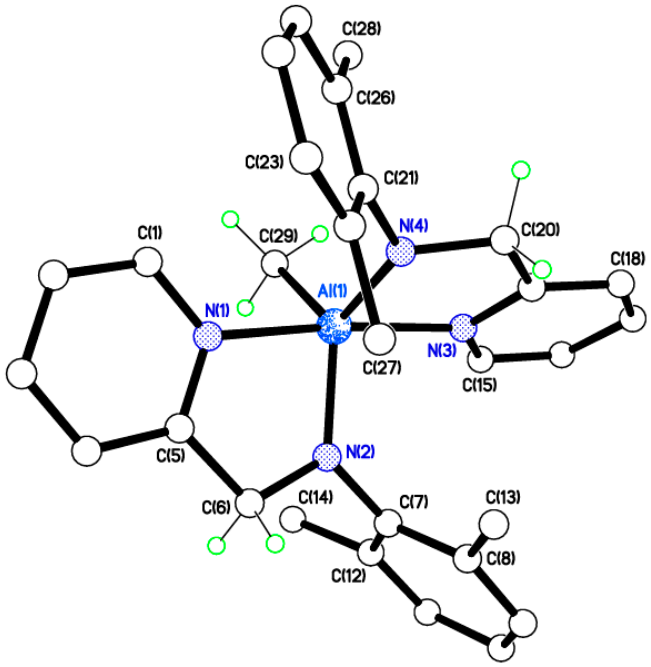

Figure 7. Molecular structure of [Al(Me)(L^1)$_2$] (**3**). Selected bond lengths (Å) and bond angles (°): Al(1)–N(1) 2.0698(11), Al(1)–N(2) 1.8671(11), Al(1)–N(3) 2.0811(11), Al(1)–N(4) 1.8703(11), Al(1)–C(29) 1.9982(13); N(1)–Al(1)–N(2) 81.45(4), N(3)–Al(1)–N(4) 81.12(4), N(1)–Al(1)–C(29) 93.65(5).

3. Ring Opening Polymerization (ROP)

3.1. Ring Opening Polymerization of ε-Caprolactone (ε-CL)

Complexes **1**–**3** and the parent compounds L^1H and L^2H have been screened for their ability to act as catalysts for the ROP of ε-caprolactone (ε-CL), and the results are

presented in Table 1. Runs were recorded at both 50 °C and 80 °C, and it was evident that better conversions were achieved at the elevated temperature. For example, at 80 °C over 30 min, the conversions observed for **1** (98%, run 5), **2** (77%, run 11) and **3** (81%, run 20), are somewhat higher than those observed at 50 °C over the same time period (34% for **1**, run 3; 11% for **2**, run 7, 5.8% for **3**, run 15). The molecular weights (M_n) of the products were higher at the elevated temperatures albeit with similar control, i.e., narrow polydispersities (M_w/M_n = Đ = 1.17–1.33). A ^{13}C NMR spectrum of a representative sample of PCL is provided in the SM (Figure S7).

Table 1. The ROP of ε-CL catalysed by **1**–**3**, L^1H and L^2H [a].

Entry	Cat. (μmol)	Temp. (°C)	Time (min)	Conv. [b] (%)	$M_{n(GPC)}$ [c] $\times 10^{-4}$	$M_{n(calc)}$ [d] $\times 10^{-4}$	M_w/M_n [c]	N [e] (μmol)
1	**1** (20)	50	10	14	1.52	1.88	1.17	14.9
2	**1** (20)	50	20	25	1.80	3.30	1.20	13.2
3	**1** (20)	50	30	34	1.50	5.26	1.30	13.2
4	**1** (20)	50	40	48	2.98	6.28	1.31	15.6
5	**1** (20)	80	30	98	9.51	12.4	1.23	16.1
6	**2** (20)	50	20	5.9	0.43	1.15	1.33	7.94
7	**2** (20)	50	30	11	0.61	1.52	1.25	10.6
8	**2** (20)	50	40	14	1.23	2.06	1.20	11.4
9	**2** (20)	50	60	17	1.11	2.46	1.27	13.8
10	**2** (20)	50	90	28	2.27	3.51	1.17	16.3
11	**2** (20)	80	30	77	3.66	8.98	1.15	17.5
12	**2** (20)	80	60	>99	6.72	11.0	1.16	18.4
13	**3** (20)	50	10	0.89	0.05	trace	-	-
14	**3** (20)	50	20	2.5	0.13	trace	-	-
15	**3** (20)	50	30	5.8	0.31	0.49	1.05	24.3
16	**3** (20)	50	40	11	0.60	1.25	1.04	17.4
17	**3** (20)	50	50	18	0.95	1.83	1.05	20.1
18	**3** (20)	50	60	25	1.39	2.77	1.06	18.6
19	**3** (20)	50	90	51	2.98	5.62	1.05	18.6
20	**3** (20)	80	30	81	3.46	7.81	1.08	21.1
21	**3** (20)	80	60	98	4.45	9.93	1.16	20.1
22	L^1H (40)	80	60	trace	-	-	-	-
23	L^2H (40)	80	60	trace	-	-	-	-

[a] Conditions: Al (20, 40 μmol), $PhCH_2OH$ (20, 40 μmol, 1 eq.), VL (10 mmol) (VL/Al = 500, 250). [b] Determined by NMR spectra. [c] Determined by GPC in $CHCl_3$ vs. polystyrene standards; Mn corrected = 0.56 × Mn obsd. [d] Calculated values of molecular weight (moles of monomer/N) × 114.14 + 108.14. [e] Estimated number of polymer chains (μmol) mass of CL reacted (mg) based on conversion/{*M*n (GPC) × 0.56} [35,36].

Kinetics

As shown in Figure 8a, the monomer consumption rate showed first order dependence toward the monomer concentration, expressed as [CL], suggesting that these ROPs by **1**–**3** proceeded without catalyst decomposition. Moreover, linear relationships between M_n values in the resultant polymer vs. polymer yield (conversion of CL) were demonstrated in Figure 8b, whereas the PDI (M_w/M_n) values were low in all cases, strongly suggesting that the ROPs proceeded in a living manner.

To further verify the end groups present, the PCL samples were analysed by MALDI-ToF mass spectrometry. Representative examples are shown in Figures 9 and 10 (see also Figure S8, SM), and in each case, one main family of polymers was evident as sodium adducts with end groups comprising OBn/OH.

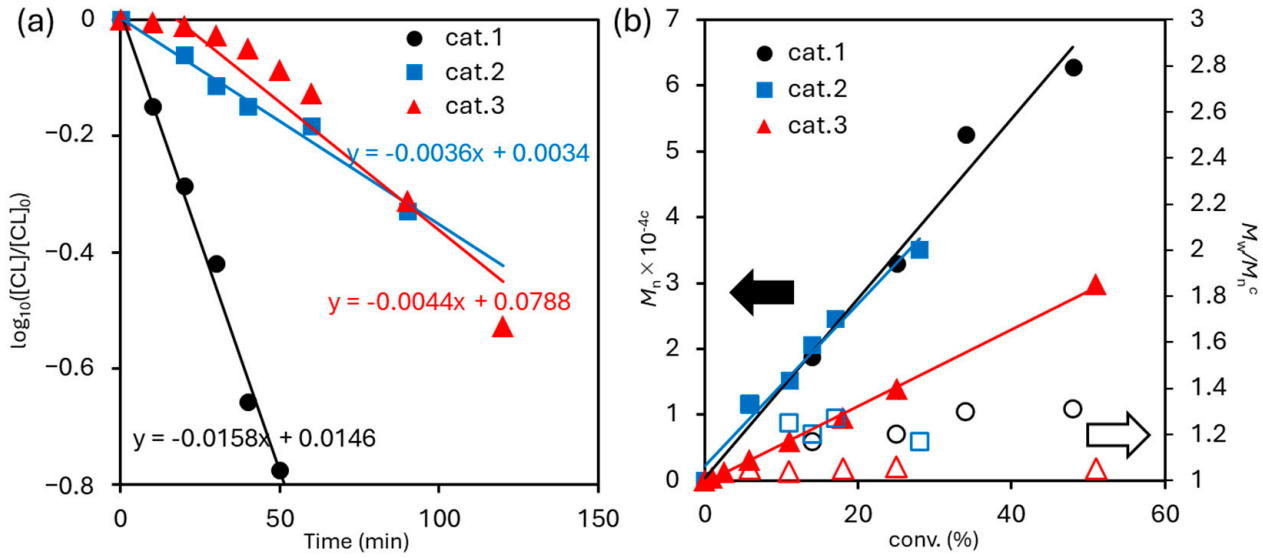

Figure 8. (**a**) Time course plots of $\log_{10}[CL]/[CL]_0$. [CL] = concentration of CL in mmol mL^{-1}. The conditions are described in Table 1 (polymerization at 50 °C, runs 1–5; runs 6–10; run 13–19). (**b**) M_n and M_w/M_n vs monomer conversion in the ROP of ε-caprolactone initiated by $\mathbf{L^1AlMe_2}$/BnOH (cat. **1**); $\mathbf{L^2AlMe_2}$/BnOH (cat. **2**) and $\mathbf{L^1{}_2AlMe_2}$/BnOH (cat. **3**) catalyst systems. The detailed conditions are summarised in Table 1.

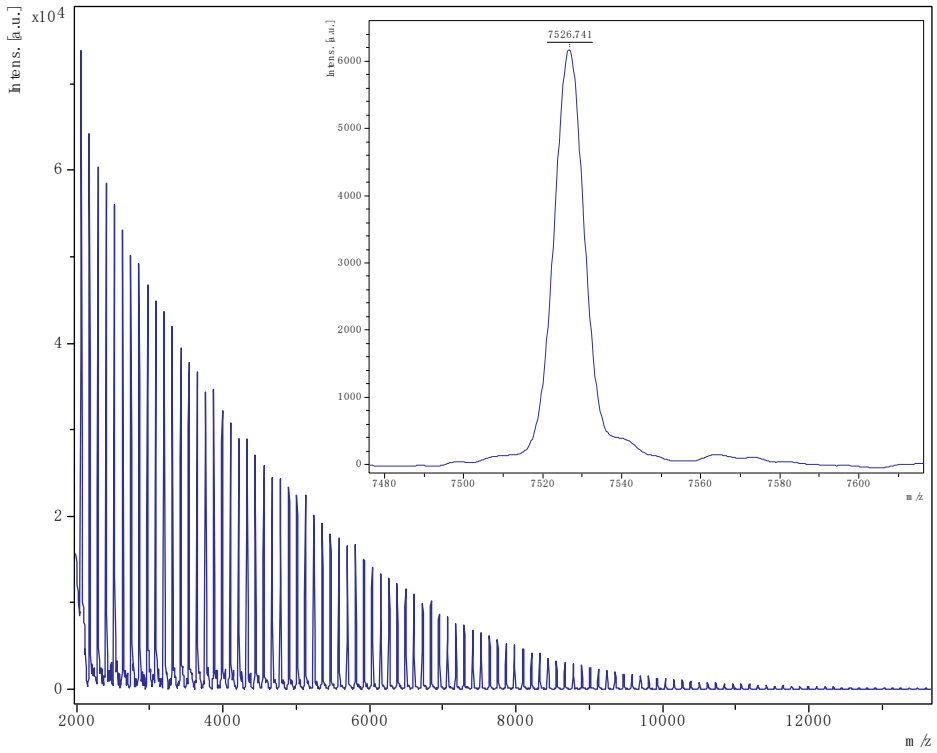

Figure 9. PCL obtained from run 4 (Table 1). The main family is chain polymer terminated by OH and BnO end groups); [M = 107.13 (OBn) + 1.008 (H) + n × 114.14 (CL) + 22.99 (Na)] (e.g., for n = 65, calc. 7527.2 obsv. 7526.7).

Given the interest in transition metal-free ROP catalysts [37], the parent pyridylamines were also screened under more robust conditions (80 °C over 1 h, see runs 22 and 23, Table 1). However, little or no polymer was obtained.

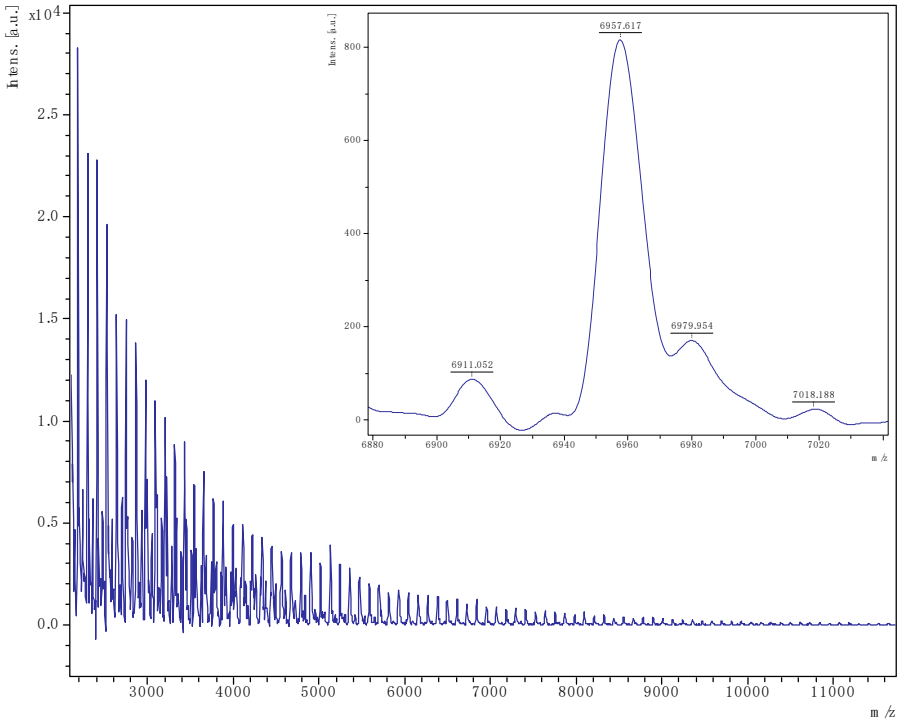

Figure 10. PCL obtained from run 12 (Table 1). The main family is chain polymer terminated by OH and BnO end groups); [M = 107.13 (OBn) + 1.008 (H) + n × 114.14 (CL) + 22.99 (Na)] (e.g., for n = 60, calc. 6956.5 obsv. 6957.6).

3.2. δ-Valerolactone (δ-VL)

Data for the ROP of δ-VL is presented in Table 2. Runs were recorded at 50 °C, and for **1** it was evident that best results were obtained for a catalyst loading of 40 μmol for ≥30 min (runs 16–18, Table 2). Under similar conditions, conversions using **2** were similar (runs 19, 20, Table 2); however, the observed molecular weights (M_n) were somewhat lower. Also, in the case of **3**, conversions were comparable over 60 min (run 32), though somewhat lower over 30 min (run 31); in each case, molecular weights (M_n) were lower than those observed for **1** and **2**. A ^{13}C NMR spectrum of a representative sample of PVL is provided in the SM (Figure S9).

Table 2. The ROP of δ-VL catalysed by **1–3**.

Run [a]	Cat. (μmol)	Temp. (°C)	Time (min)	Conv. [b] (%)	$M_{n(GPC)}$ [c] $\times 10^{-4}$	$M_{n(calc)}$ [d] $\times 10^{-4}$	M_w/M_n [c]	N [e] (μmol)
24	**1** (20)	50	60	22	1.23	4.94	1.05	20.3
25	**1** (40)	50	10	59	1.60	2.40	1.12	41.9
26	**1** (40)	50	30	88	2.46	2.48	1.13	40.6
27	**1** (40)	50	50	93	2.50	2.37	1.2	42.4
28	**1** (40)	50	60	93	2.52	2.39	1.2	42
29	**2** (40)	50	30	83	2.43	2.53	1.48	39.7
30	**2** (40)	50	60	92	3.00	2.88	1.4	34.9
31	**3** (40)	50	30	62	0.91	1.47	1.11	68.4
32	**3** (40)	50	60	91	1.72	1.90	1.12	52.9

[a] Conditions: Al (20, 40 μmol), $PhCH_2OH$ (20, 40 μmol, 1 eq.), VL (10 mmol) (VL/Al = 500, 250). [b] Determined by NMR spectra. [c] Determined by GPC in $CHCl_3$ vs. polystyrene standards; Mn corrected = 0.57 × Mn obsd. [d] Calculated values of molecular weight (moles of monomer/N) × 100.12 + 108.14. [e] Estimated number of polymer chains (μmol) mass of CL reacted (mg) based on conversion/{*M*n (GPC) × 0.57} [35,36].

As for ε-CL, use of either L^1H or L^2H with δ-VL under more robust conditions (80 °C) failed to afford any polymeric products.

3.2.1. Kinetics

As demonstrated in the ROP of CL, the monomer consumption rate in ROP of VL showed first order dependence toward the monomer concentration (Figure 11a), expressed as [VL], suggesting that these ROPs by **1** (and maybe **2**) proceeded without catalyst decomposition. As shown in Figure 11b, a linear correlation between M_n values in the resultant polymer vs. polymer yield (conversion of VL) by catalyst **1** suggests a quasi-living nature of the ROP.

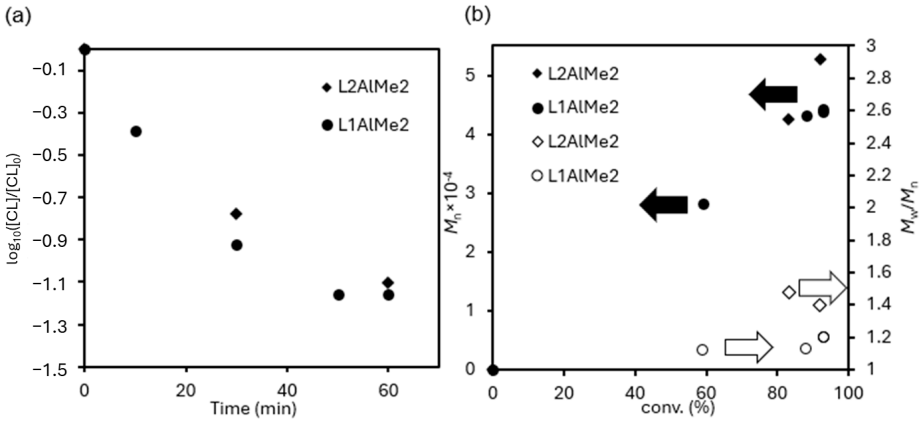

Figure 11. (**a**) Time course plots of $\log_{10}[VL]/[VL]_0$. [VL] = concentration of VL in mmol mL^{-1}. The conditions are described in Table 1 (polymerization at 50 °C, runs 15–19; runs 20–21). (**b**) M_n and M_w/M_n vs monomer conversion in the ring opening polymerization of ε-caprolactone initiated by $\mathbf{L^1AlMe_2}$/BnOH (**1**; •,○); $\mathbf{L^2AlMe_2}$/BnOH (**2**; υ,◇) catalyst systems. The detailed conditions are summarised in Table 2.

3.2.2. MALDI-ToF Spectra

As for the PCL, analysis of the polymers by MALDI-ToF (Figures 12 and 13, see also Figure S10, SM) revealed the formation of chain polymers with end groups comprising OBn/OH.

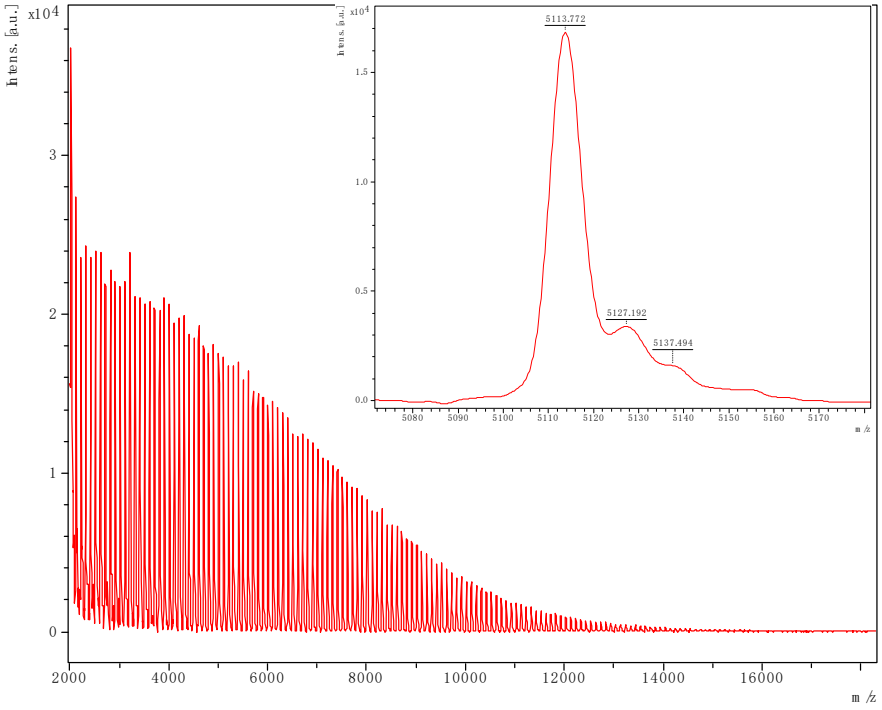

Figure 12. PVL obtained from run 25 (Table 2). The main family is chain polymer terminated by OH and BnO end groups); [M = 107.13 (OBn) + 1.008 (H) + n × 100.11 (VL) + 22.99 (Na)] (e.g., for n = 50, calc. 5113.6 obsv. 5113.8).

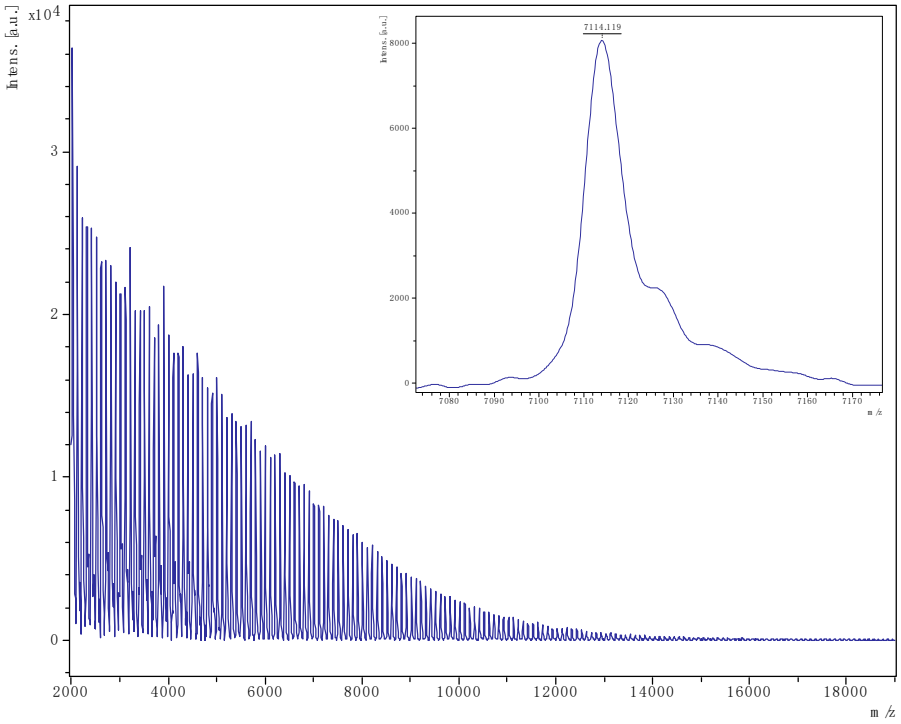

Figure 13. PVL obtained from run 26 (Table 2). The main family is chain polymer terminated by OH and BnO end groups); [M = 107.13 (OBn) + 1.008 (H) + n × 100.11 (VL) + 22.99 (Na)] (e.g., for n = 70, calc. 7114.1, obsv. 7114.1).

4. Experimental

4.1. General

The reactions were conducted under a nitrogen atmosphere using standard Schlenk techniques unless specified otherwise. Toluene was dried over sodium, acetonitrile dried over calcium hydride, and solvents were degassed prior to use. The known compound L^1H was prepared using the method proposed in the literature [26]. The reagent Me_3Al was purchased from Sigma Aldrich (Gillingham, UK) and was used as received. ε-Caprolactone (Fisher Scientific, Loughborough, UK) and δ-valerolactone (Sigma Aldrich, Gillingham, UK) were dried (CaH_2) and distilled prior to use. NMR spectra were recorded at 400.2 MHz on a JEOL ECZ 400S spectrometer (Peabody, MA, USA), using residual protic solvent as the internal standard. Chemical shifts are provided in ppm (δ) with coupling constants (*J*) given in Hertz (Hz). Combustion analyses were performed by the elemental analysis service at London Metropolitan University or the Xi'an Rare Metal Materials Research Institute Co., Ltd. Matrix Assisted Laser Desorption/Ionisation Time of Flight (MALDI-TOF) mass spectrometry was performed using a Bruker autoflex III Smart beam in linear mode, and the spectra were acquired by averaging at least 100 laser shots. The matrix used was 2,5-dihydroxybenzoic acid with THF as the solvent. The ionising agent used was sodium chloride dissolved in methanol. Samples were prepared by mixing 20 μL of matrix solution in THF (2 mg·mL^{-1}) with 20 μL of matrix solution (10 mg·mL^{-1}) and 1 μL of a solution of ionising agent (1 mg·mL^{-1}). Following this, 1 mL of these mixtures was deposited on a target plate and allowed to dry under air at ambient temperature. OmniSEC software (Malvern Panalytical Ltd., Malvern, UK, v11.35) was used to calculate the molecular weights from the experimental traces.

4.1.1. Synthesis of $\mathbf{L^2H}$

A mixture of 1-(pyridin-2-yl)ethan-1-one (7.60 g, 62.7 mmol), 2,6-dimethylaniline (7.55 g, 62.3 mmol) and *p*-toluenesulfonic acid (615 mg, 3.24 mmol) in toluene (30 mL) was

refluxed for 16 h. On cooling, the reaction mixture was then extracted with AcOEt and washed with brine. The organic layer was dried over Na_2SO_4 and the solvent removed under vacuum, to afford 11.7 g (52.2 mmol, 83%) of the intermediate. $AlMe_3$ (12.5 mL, 25.0 mmol, 2M solution) was added to the resulting intermediate (5.00 g, 22.3 mmol) in toluene (120 mL) and the system was refluxed for 4 h. The reaction mixture was quenched with 3M NaOH aq. at 0 °C and then extracted with AcOEt and washed with brine. After the solvent was removed from the organic layer under vacuum, the crude product was purified using silica gel chromatography (AcOEt/Hex 4/1). L^2H was obtained as orange oil. Yield: 3.63 g, 68%. ^{1}H NMR (500 MHz, C_6D_6 298 K) δ: 8.46 (m, 1H, aryl*H*), 7.36 (m, 1H, aryl*H*), 7.13 (m, 2H, aryl*H*), 7.10 (m, 1H, aryl*H*), 6.63 (m, 1H, aryl*H*), 4.09 (s, 1H, N-H), 2.07 (s, 6H, *o*-CH_3), 1.50 (s, 6H, C-*Me*$_2$).

4.1.2. Synthesis of [$Me_2Al(L^1)$] (**1**)

To L^1H (1.00 g, 4.71 mmol) in toluene (20 mL) was added the $AlMe_3$ (2.83 mL, 5.66 mmol, 2M solution) and the system was refluxed for 18 h. On cooling, the volatiles were removed in vacuo, and the residue was extracted into MeCN (20 mL). Standing at 0 °C afforded **1** as colourless prisms. Yield: 0.77 g, 61%. Found: C 71.39, H 7.90, N 10.83%. $C_{16}H_{21}AlN_2$ requires C 71.62, H 7.89, N 10.44%. ^{1}H NMR (400 MHz, C_6D_6, 298 K) δ: 7.58 (m, 1H, aryl*H*), 7.22 (d, *J* = 7.3 Hz, 2H, aryl*H*), 7.08 (t, *J* = 7.2 Hz, 1H, aryl*H*), 6.68 (m, 1H, aryl*H*), 6.37 (overlapping m, 2H, aryl*H*), 4.37 (s, 2H, CH_2), 2.48 (s, 6H, *o*-CH_3), −0.27 (s, 6H, Al-CH_3).

4.1.3. Synthesis of [$Me_2Al(L^2)$] (**2**)

As for **1**, but using L^2H (1.00 g, 4.16 mmol) and $AlMe_3$ (2.50 mL, 2 M, 5.00 mmol), affording **2** as colourless prisms. Yield: 1.13 g, 92%. Found: C 72.56, H 8.68, N 9.40%. $C_{18}H_{25}AlN_2$ requires C 72.94, H 8.50, N 9.45%. ^{1}H NMR (400 MHz, C_6D_6, 298 K) δ: 7.60 (m, 1H, aryl*H*), 7.25 (d, *J* = 7.2 Hz, 2H, aryl*H*), 7.06 (t, *J* = 7.0 Hz, 1H, aryl*H*), 6.82 (m, 1H, aryl*H*), 6.68 (m, 1H, aryl*H*), 6.29 (m, 1H, aryl*H*), 2.48 (s, 6H, *o*-CH_3), 1.27 (s, 6H C*Me*$_2$), −0.28 (s, 6H, Al-CH_3).

4.1.4. Synthesis of [$MeAl(L^1)_2$] (**3**)

As for **1**, but L^1H (2.00 g, 9.42 mmol) in toluene (20 mL) was added to $AlMe_3$ (2.25 mL, 4.50 mmol, 2M solution), which afforded **3** as colourless blocks. Yield: 1.69 g, 81%. Found: C 73.55, H 7.25, N 12.23%. $C_{29}H_{33}AlN_4$ requires C 74.97, H 7.16, N 12.06%. ^{1}H NMR (400 MHz, C_6D_6, 298 K) δ: 7.40 (m, 1H, aryl*H*), 7.17 (m, 2H, aryl*H*), 6.86 (m, 3H, aryl*H*), 6.73 (m, 2H, aryl*H*), 6.65 (m, 2H, aryl*H*), 6.41 (overlapping m, 2H, aryl*H*), 6.10 (overlapping m, 2H, aryl*H*), 4.49 (d, *J* = 20.0 Hz, 2H, CH_2), 4.29 (d, *J* = 20.0 Hz, 2H, CH_2), 2.57 (s, 6H, *o*-CH_3), 2.02 (s, 6H, *o*-CH_3), −0.28 (s, 3H, Al-CH_3).

4.2. Procedure for ROP of ε-Caprolactone or δ-Valerolacone

A toluene solution of pre-catalyst (0.010 mmol, 1.0 mL toluene) was added into a Schlenk tube in the glovebox at room temperature. The solution was stirred for 2 min, and then the appropriate equivalent of BnOH (from a pre-prepared stock solution of 1 mmol BnOH in 100 mL toluene) and the appropriate amount of ε-CL (or δ-VL), along with 1.5 mL toluene, was added to the solution. For example, for Table 2, entry 1, a toluene solution of pre-catalyst **1** (0.010 mmol, 1.0 mL toluene) was added into a Schlenk tube, then 2 mL BnOH solution (1 mmol BnOH/100 mL toluene) and 20 mmol ε-CL along with 1.5 mL toluene was added to the solution. The reaction mixture was then placed into an oil/sand bath pre-heated at 130 °C, and the solution was stirred for the prescribed time (24 h). The polymerization mixture was quenched on addition of an excess of glacial acetic acid

(0.2 mL) to the solution, and the resultant solution was then poured into methanol (200 mL). The resultant polymer was then collected on filter paper and was dried in vacuo.

4.2.1. Kinetic Studies

The polymerizations were carried out at 130 °C in toluene (2 mL) using 0.010 mmol of complex. The molar ratio of monomer to initiator was fixed at 500:1, and at appropriate time intervals, 0.5 µL aliquots were removed (under N_2) and were quenched with wet $CDCl_3$. The percent conversion of monomer to polymer was determined using ^{1}H NMR spectroscopy.

4.2.2. Crystallography

Diffraction data for **1**–**3** were collected at low temperature on rotating-anode Rigaku XtalLAB AFC11 (RCD3), FRE+ or 007HF diffractometers, respectively, equipped with HyPix detectors (Neu-Isenberg, Germany). The data were corrected for Lp effects and absorption. All structures were solved via dual-space, iterative, charge-flipping methods [38] and refined routinely on F^2 values [39]. Further details are given in Table 3 below. CCDC, 2414170 {**1**}, 2385189 {2} and 2385188 {**3**} contain the supplementary crystallographic data for this paper. These data can be obtained free of charge from The Cambridge Crystallographic Data Centre via www.ccdc.cam.ac.uk/structures (accessed on 10 November 2025).

Table 3. Crystallographic data for **1**–**3**.

Compound	**1**	**2**	**3**
Formula weight	268.33	296.38	464.57
Crystal system	Orthorhombic	Orthorhombic	Monoclinic
Space group	*Pbca*	*Pnma*	$P2_1/c$
Unit cell dimensions			
a (Å)	14.8183(2)	16.71447(18)	15.36793(12)
b (Å)	12.9284(2)	11.79057(15)	8.16407(6)
c (Å)	32.4960(5)	8.71683(10)	21.64688(17)
β (°)	90	90	110.0738(9)
V (Å^3)	6225.48(16)	1717.85(3)	2550.93(4)
Z	16	4	4
Temperature (K)	93(2)	100(2)	100(2)
Wavelength (Å)	1.54184	0.71073	1.54178
Calculated density (g.cm^{-3})	1.145	1.146	1.210
Absorption coefficient (mm^{-1})	1.03	0.11	0.87
Transmission factors (min./max.)	0.709 and 1.000	0.928 and 1.000	0.808 and 1.000
Crystal size (mm^3)	0.27 × 0.09 × 0.06	0.20 × 0.08 × 0.07	0.22 × 0.20 × 0.05
θ(max) (°)	73.7	36.0	73.5
Reflections measured	38,334	69,199	84,510
Unique reflections	6191	4115	4918
R_{int}	0.074	0.024	0.024
Reflections with $F^2 > 2\sigma(F^2)$	4632	3717	4850
Number of parameters	352	115	313
R_1 [$F^2 > 2\sigma(F^2)$]	0.068	0.034	0.034
wR_2 (all data)	0.136	0.102	0.087
GOOF, S	1.03	1.05	1.05
Largest difference peak and hole (e Å^{-3})	0.34 and −0.30	0.47 and −0.23	0.26 and −0.24

5. Conclusions

The pyridylamines 2,6-$Me_2C_6H_3NHCR_2$-C_5H_5H-2 (R = H, L^1H; Me, L^2H) upon reaction with equimolar amounts of Me_3Al undergo a methyl transfer to the imine backbone to afford the complexes $[Al(Me)_2(L^1)]$ (**1**) and $[Al(Me)_2L^2]$ (**2**) in good yield (>90%). Use of excess L^1H led to the isolation of the bis-chelate complex $[Al(Me)(L^1)_2]$ (**3**). These aluminium-based systems are active as catalysts for the ROP of ε-caprolactone and δ-valerolactone when employed in solution (toluene) under N_2. The products are of medium to high molecular weight for PCL (1.15–12.4 × 10^4 Da) and medium molecular weight for PVL (1.59–5.27 × 10^4 Da), and generally have narrow Đ (1.15–1.33 for PCL; 1.05–1.48 for PVL). MALDI-ToF mass spectra of the polymers indicated that linear polymers with BnO/H end groups were formed. Kinetic profiles revealed the living nature of the process without catalyst deactivation. Whilst direct comparisons with the majority of the pyridyl-alkylamide aluminium catalysts bearing naphthyl substituents (see **I** and **II**, Figure S1, SM) mentioned earlier are not possible given the differing ROP conditions, we note that the system bearing **II** (R = *i*Pr) was screened at 50 °C over 30 and 60 min (250:1:1 for ε-CL:Al:BnOH in toluene) which afforded conversions of 86 and 100%, respectively. The catalysts herein only matched such conversions at 80 °C. In terms of the products formed, the naphthyl complexes afforded PCL with M_n 20270 Da (30 min) and 28880 Da (60 min), which are results comparable with those observed for **1** (see entries 3 and 4, Table 1) at the same temperature, whilst the control, as evidenced by the Đ values, was better in the case of **1**. The parent compounds L^1H and L^2H used in this work were virtually inactive for the ROP of ε-CL and δ-VL under the conditions employed.

Supplementary Materials: The following supporting information can be downloaded at https://www.mdpi.com/article/10.3390/catal15121119/s1: Figure S1, Literature compounds **I–VI**. Figures S2–S4, ^{1}H NMR spectrum of complexes **1–3** (400 MHz in C_6D_6 at 20 °C. Figures S5–S6, Additional figures for crystallographic analysis of **2**. Figures S7–S9, ^{13}C NMR spectra of representative polymers, Figures S8–S10, MALDI-ToF spectra of ring opened polymers.

Author Contributions: S.S.: Investigation. I.M.: Investigation. M.R.J.E.: Investigation, Writing—review and editing. K.N.: Conceptualization, Supervision, Writing—original draft, Writing—review and editing. C.R.: Conceptualization, Supervision, Writing—original draft, Writing—review and editing. All authors have read and agreed to the published version of the manuscript.

Funding: We thank the Royal Society for support (grant number IECR32113010).

Data Availability Statement: Data are contained within the article and Supplementary Materials.

Conflicts of Interest: The authors declare that they have no known competing financial interests or personal relationships that could have appeared to influence the work reported in this paper.

References

1. Labet, M.; Thielemans, W. Synthesis of polycaprolactone: A review. *Chem. Soc. Rev.* **2009**, *38*, 3484–3504. [CrossRef]
2. Arbaoui, A.; Redshaw, C. Metal Catalysts for ε-caprolactone polymerisation. *Polym. Chem.* **2010**, *1*, 801–826. [CrossRef]
3. Thomas, C.M. Stereo-controlled ring-opening polymerization of cyclic esters: Synthesis of new polyester microstructures. *Chem. Soc. Rev.* **2010**, *39*, 165–173. [CrossRef]
4. Gao, J.; Zhu, D.; Zhang, W.; Solan, G.A.; Ma, Y.; Sun, W.-H. Recent progress in the application of group 1, 2 & 13 metal complexes as catalysts for the ring opening polymerization of cyclic esters. *Inorg. Chem. Front.* **2019**, *6*, 2619–2652. [CrossRef]
5. Santoro, O.; Zhang, X.; Redshaw, C. Synthesis of biodegradable polymers: A review on the use of Schiff-base metal complexes as catalysts for the Ring Opening Polymerization (ROP) of cyclic esters. *Catalysts* **2020**, *10*, 800. [CrossRef]
6. Wu, L.-J.; Lee, W.; Ganta, P.K.; Chang, Y.-L.; Chang, Y.-C.; Chen, H.-Y. Multinuclear metal catalysts in ring-opening polymerization of ε caprolactone and lactide: Cooperative and electronic effects between metal centers. *Coord. Chem. Rev.* **2023**, *475*, 214847. [CrossRef]
7. D'Auria, I.; D'Alterio, M.C.; Tedesco, C.; Pellecchia, C. Tailor-made block copolymers of L-, D- and *rac*-lactides and e-caprolactone via one-pot sequential ring opening polymerization by pyridylamidozinc(II) catalysts. *RSC Adv.* **2019**, *9*, 32771–32779. [CrossRef] [PubMed]

8. Bhattacharjee, J.; Sarker, A.; Panda, T.K. Alkali and alkali earth metal complexes as versatile catalysts for ring-opening polymerization of cyclic esters. *Chem. Rec.* **2021**, *21*, 1898–1911. [CrossRef]
9. Hashmi, O.H.; Capet, F.; Visseaux, M.; Champouret, Y. Homoleptic and heteroleptic substituted amidomethylpyridine iron complexes: Synthesis, structure and polymerization of *rac*-lactide. *Eur. J. Inorg. Chem.* **2022**, *2022*, e2022000073. [CrossRef]
10. Wang, Y.; Wang, X.; Zhang, W.; Sun, W.-H. Progress of ring-opening polymerization of cyclic esters by iron compounds. *Organometallics* **2023**, *42*, 1680–1692. [CrossRef]
11. Gravina, G.; Pierri, G.; Pellecchia, C. New highly acive Fe(II) pyridylamido catalyst for the ring opening polymerization and copolymerization of cyclic esters. *Mol. Catal.* **2024**, *555*, 113891. [CrossRef]
12. Iwasa, N.; Fujiki, M.; Nomura, K. Ring-opening polymerization of various cyclic esters by Al complex catalysts containing a series of phenoxy-imine ligands: Effect of the imino substituents for the catalytic activity. *J. Mol. Catal. A Chem.* **2008**, *292*, 67–75. [CrossRef]
13. Iwasa, N.; Katao, S.; Liu, J.; Fujiki, M.; Furukawa, Y.; Nomura, K. Notable effect of fluoro substituents in the imino group in ring-opening polymerization of ε-caprolactone by Al complexes containing phenoxyimine ligands. *Organometallics* **2009**, *28*, 2179–2187. [CrossRef]
14. Liu, J.; Iwasa, N.; Nomura, K. Synthesis of Al complexes containing phenoxy-imine ligands and their use as the catalyst precursors for efficient living ring-opening polymerisation of ε-caprolactone. *Dalton Trans.* **2008**, 3978–3988. [CrossRef]
15. Li, Y.; Zhao, K.-Q.; Elsegood, M.R.J.; Prior, T.J.; Sun, X.; Mo, S.; Redshaw, C. Organoaluminium complexes of *o*-,*m*-,*p*-anisidines: Synthesis, structural studies and ROP of ε-caprolactone. *Cat. Sci. Tech.* **2014**, *4*, 3025–3031. [CrossRef]
16. Fuoco, T.; Pappalardo, D. Alkyl aluminum complexes bearing salicylaldiminato ligands: Initiators in the ring-opening polymerization of cyclic esters. *Catalysts* **2017**, *7*, 64. [CrossRef]
17. Wang, K.; Zhao, K.-Q.; Mo, S.; Al-Khafaji, Y.; Prior, T.J.; Elsegood, M.R.J.; Redshaw, C. Organoaluminium complexes derived from Anilines or Schiff bases for ring opening polymerization of ε-caprolactone, δ-valerolactone and rac-lactide. *Eur. J. Inorg. Chem.* **2017**, *2017*, 1951–1965. [CrossRef]
18. García-Valle, F.M.; Cuenca, T.; Mosquera, M.E.G.; Millone, S.; Cano, J. Ring-opening polymerization (ROP) of cyclic esters by versatile aluminum diphenoxyimine complexes: From polylactide to random copolymers. *Eur. Polym. J.* **2020**, *125*, 109527. [CrossRef]
19. Jiang, Y.; Zhang, W.; Han, M.; Wang, X.; Solan, G.A.; Wang, R.; Ma, Y.; Sun, W.-H. Phenoxy-imine/-amide aluminum complexes with pendant or coordinated pyridine moieties: Solvent effects on structural type and catalytic capability for the ROP of cyclic esters. *Polymer* **2022**, *242*, 124602. [CrossRef]
20. Sagar, S.; Nath, P.; Bano, K.; Karmakar, H.; Sharma, J.; Sarkar, A.; Panda, T.K. Binunclear and mononuclear aluminum complexes as quick and controlled initiators of well-orderd ROP of cyclic esters. *ChemCatChem* **2024**, *16*, e202300972. [CrossRef]
21. Sumrit, P.; Kamavichanurat, S.; Joopor, W.; Wattanathana, W.; Nakornkhet, C.; Hormnirun, P. Aluminium complexes of phenoxy-azo ligands in the catalysis of rac-lactide polymerisation. *Dalton Trans.* **2024**, *53*, 13854–13870. [CrossRef] [PubMed]
22. García-López, J.D.; García-Álvarez, A.-C.; Hernández-Balderas, U.; Gallardo-Garibay, A.; Jancik, V.; Martínez-Otero, D.; Moya-Cabrera, M. Ligand-directed assembly of multimetallic aluminum complexes: Synthesis, structure and ROP catalysis. *Eur. J. Inorg. Chem.* **2024**, *27*, e202400466. [CrossRef]
23. Annunziata, L.; Pragliola, S.; Pappalardo, D.; Tedesco, C.; Pellecchia, C. New (anilidomethyl)pyridine Titanium(IV) and Zirconium(IV) catalyst precursors for the Highly Chemo- and Stereoselective cis-1,4-polymerization of 1,3-buadiene. *Macromolecules* **2011**, *44*, 1934–1941. [CrossRef]
24. Zhang, S.; Katao, S.; Sun, W.-H.; Nomura, K. Synthesis of (arylimido)vanadium(V) complexes containing (2-anilidomethyl)pyridine ligands and their use as the catalyst precursors for olefin polymerization. *Organometallics* **2009**, *28*, 5925–5933. [CrossRef]
25. Zhang, S.; Nomura, K. Highly efficient dimerization of ethylene by (imido)vanadium complexes containing (2-anilidomethyl)pyridine ligand: Notable ligand effect toward activity and selectivity. *J. Am. Chem. Soc.* **2010**, *132*, 4960–4965. [CrossRef]
26. Nomura, K.; Mitsudome, T.; Igarashi, A.; Nagai, G.; Tsutsumi, K.; Ina, T.; Omiya, T.; Takaya, H.; Yamazoe, S. Synthesis of (Adamantylimido)vanadium(V) Dimethyl Complex Containing (2-Anilidomethyl)pyridine Ligand and Selected Reactions: Exploring the Oxidation State of the Catalytically Active Species in Ethylene Dimerization. *Organometallics* **2017**, *36*, 530–542. [CrossRef]
27. Kuboki, M.; Nomura, K. (Arylimido)niobium(V) Complexes Containing 2-Pyridylmethylanilido Ligand as Catalyst Precursors for Ethylene Dimerization That Proceeds via Cationic Nb(V) Species. *Organometallics* **2019**, *38*, 1544–1559. [CrossRef]
28. Armitage, A.P.; Boyron, O.; Champouret, Y.D.M.; Patel, M.; Singh, K.; Solan, G.A. Dimethyl-Aluminium Complexes Bearing Naphthyl-Substituted Pyridine-Alkylamides as Pro-Initiators for the Efficient ROP of ε-Caprolactone. *Catalysts* **2015**, *5*, 1425–1444. [CrossRef]
29. Nienkemper, K.; Kehr, G.; Kehr, S.; Fröhlich, R.; Erker, G. (Amidomethyl)pyridine zirconium and hafnium complexes: Synthesis and structural characterization. *J. Organomet. Chem.* **2008**, *693*, 1572–1589. [CrossRef]
30. Knijnenburg, Q.; Smits, J.M.M.; Budzelaar, P.H.M. Reaction of the Diimine Pyridine Ligand with Aluminum Alkyls: An Unexpectedly Complex Reaction. *Organometallics* **2006**, *25*, 1036–1046. [CrossRef]

31. Davies, C.J.; Gregory, A.; Griffith, P.; Perkins, T.; Singh, K.; Solan, G.A. Use of Suzuki cross-coupling as a route to 2-phenoxy-6-iminopyridines and chiral 2-phenoxy-6-(methanamino) pyridines. *Tetrahedron* **2008**, *64*, 9857–9864. [CrossRef]
32. Wei, Y.; Wang, S.; Zhou, S.; Feng, Z.; Guo, L.; Zhu, X.; Mu, X.; Yao, F. Aluminum Alkyl Complexes Supported by Bidentate *N*,*N* Ligands: Synthesis, Structure, and Catalytic Activity for Guanylation of Amines. *Organometallics* **2015**, *34*, 1882–1889. [CrossRef]
33. Liu, R.; Yang, S.; Ding, Y.; Xia, D. Study on the effect of substituents on the structure, volatility, and fluorescence of *N*-(Alkyl or TMS)-2-pyridinamine diethyl aluminum complexes. *J. Organomet. Chem.* **2021**, *933*, 121646. [CrossRef]
34. Addison, A.W.; Rao, T.N.; Reedijk, J.; van Rijn, J.; Verschoor, G.C. Synthesis, structure, and spectroscopic properties of copper(II) compounds containing nitrogen–sulphur donor ligands; the crystal and molecular structure of aqua[1,7-bis(*N*-methylbenzimidazol-2′-yl)-2,6-dithiaheptane]copper(II) perchlorate. *J. Chem. Soc. Dalton Trans.* **1984**, 1349–1356. [CrossRef]
35. Huang, C.-H.; Wang, F.-C.; Ko, B.-T.; Yu, T.-L.; Lin, C.-C. Ring-Opening Polymerization of ε-Caprolactone and L-Lactide Using Aluminum Thiolates as Initiator. *Macromolecules* **2001**, *34*, 356–361. [CrossRef]
36. Save, M.; Schappacher, M.; Soum, A. Controlled Ring-Opening Polymerization of Lactones and Lactides Initiated by Lanthanum Isopropoxide, 1. General Aspects and Kinetics. *Macromol. Chem. Phys.* **2002**, *203*, 889–899. [CrossRef]
37. Dove, A.P. Organic Catalysis for Ring Opening Polymerization. *ACS Macro Lett.* **2012**, *1*, 1409–1412. [CrossRef]
38. Sheldrick, G.M. SHELXT–Integrated space-group and crystal structure determination. *Acta Cryst.* **2015**, *A71*, 3–8. [CrossRef]
39. Sheldrick, G.M. Crystal structure refinement with SHELXL. *Acta Cryst.* **2015**, *C71*, 3–8. [CrossRef]

Disclaimer/Publisher's Note: The statements, opinions and data contained in all publications are solely those of the individual author(s) and contributor(s) and not of MDPI and/or the editor(s). MDPI and/or the editor(s) disclaim responsibility for any injury to people or property resulting from any ideas, methods, instructions or products referred to in the content.